Available online at www.sciencedirect.com
ScienceDirect
Chinese Journal of Natural Medicines 2022, **20**(8): 601-613
doi: 10.1016/S1875-5364(22)60186-9
Chinese Journal of Natural Medicines

•Research article•

Effect of astragaloside IV and salvianolic acid B on antioxidant stress and vascular endothelial protection in the treatment of atherosclerosis based on metabonomics

KONG Xiang-Lin[1Δ], LYU Qin[2Δ], ZHANG Ya-Qi[3Δ], KANG Dong-Fang[4], LI Chao[4], ZHANG Lei[5], GAO Zi-Chen[5], LIU Xin-Xin[5], WU Ji-Biao[5*], LI Yun-Lun[4, 6*]

[1] *Experimental Center, Shandong University of Traditional Chinese Medicine, Jinan 250355, China;*
[2] *Graduate School, Liaoning University of Traditional Chinese Medicine, Shenyang 110847, China;*
[3] *College of Continuing Education, Shandong University of Traditional Chinese Medicine, Jinan, 250355, China;*
[4] *Innovative Institute of Chinese Medicine and Pharmacy, Shandong University of Traditional Chinese Medicine, Jinan 250355, China;*
[5] *College of Traditional Chinese Medicine, Shandong University of Traditional Chinese Medicine, Jinan 250355, China;*
[6] *Department of Cardiology, the Affiliated Hospital of Shandong University of Traditional Chinese Medicine, Jinan 250011, China*

Available online 20 Aug., 2022

[ABSTRACT] Vascular endothelial cells and oxidation reduction system play an important role in the pathogenesis of atherosclerosis (AS). If these conditions are disordered, it will inevitably lead to plaque formation and even rupture. Astragaloside IV (AsIV) and salvianolic acid B (Sal B) are the main active ingredients of *Astragalus membranaceus* and *Salvia miltiorrhiza*, respectively, and found to ameliorate vascular endothelial dysfunction and protect against oxidative stress in recent studies. However, it is still unknown if the combination of AsIV and Sal B (AsIV + Sal B) can inhibit the development of plaque through amplifying the protective effect of vascular endothelial cells and anti-oxidative stress effect. To clarify the role of AsIV + Sal B in AS, we observed the efficacy of each group (Control, Model, AsIV, Sal B, and AsIV + Sal B) by biomolecular assays, such as observing the pathological morphology of the aorta by oil red O staining, evaluating the level of oxidative stress and endothelial cells in the serum by the Elisa test, and analyzing the changes of all small molecule metabolites in liver tissue by UPLC-QTOF-MS. Results showed that AsIV, Sal B and AsIV + Sal B decreased the deposition of lipid in the arterial wall, so as to exert the effect of anti-oxidant stress and vascular endothelial protection, where the inhibitory effect of AsIV + Sal B was the most obvious. Metabonomics analysis showed that Sal B regulated the metabolic pathways of arginine and proline. AsIV regulated glycerol metabolism and saturated fatty acid biosynthesis metabolism. AsIV + Sal B is mainly related to the regulation of the citrate cycle (TCA cycle), alanine, aspartic acid, and glutamate metabolism, cysteine, and methionine metabolism. Succinic acid and methionine are synergistic metabolites that exert an enhancing effect when AsIV and Sal B were used in combination. In conclusion, we demonstrated that AsIV acompanied with Sal B can be successfully used for anti-oxidative stress and vascular endothelial protection of AS, and succinic acid and methionine are the synergistic metabolites.

[KEY WORDS] Salvianolic acid B; Astragaloside IV; Metabolomics; Oxidative stress; Vascular endothelial damage
[CLC Number] R965 **[Document code]** A **[Article ID]** 2095-6975(2022)08-0601-13

Introduction

Atherosclerosis (AS) is an important cause of coronary heart disease, cerebral infarction, peripheral vascular diseases and diabetes, and also the most critical pathological basis of cardiovascular disease (CVD) [1, 2], which poses a serious threat to human health [3]. At present, many scholars believe that the key problem of AS lies in the fact that early endothelial cells are susceptible to the influence of oxygen free radicals, resulting in endothelial cell damage. In addition, intravascular cholesterol and other lipids that accumulate within the vessels for a long time are easily to be oxidized. Oxidized proteins and oxidatively modified low-density lipoprotein (OX-LDL) attach to the vascular wall, and aggravate free

[Received on] 19-Feb.-2022
[Research funding] This work was supported by the National Natural Science Foundation of China (No. 81974566) and the Taishan Scholar Construction Project Grant Project (No. ts201712042).
[*]**Corresponding author]** E-mails: wujibiao1963@126.com (WU Ji-Biao); liyunlun@126.com (LI Yun-Lun)
[Δ]These authors contributed equally to this work.
These authors have no conflict of interest to declare.

radical damage, resulting in a series of pathological manifestations [4, 5]. It can be seen that oxidation and endothelial damage occur before the appearance of visible plaques, which are the main factors affecting the pathogenesis of AS [6, 7].

Traditional Chinese medicine (TCM) is derived from valuable practical experience for thousands of years. Chinese herbal medicine can effectively treat complex diseases based on its unique characteristics of "multi-component, multi-path and multi-target" [8]. According to the literature, the combination of *Astragalus membranaceus* and *Salvia miltiorrhiza* is an effective prescription that is widely used for the treatment of CVD [9-11]. Astragaloside IV (AsIV) and salvianolic acid B (Sal B) are the active components of *Astragalus membranaceus* and *Salvia miltiorrhiza*, respectively. Studies have shown that AsIV and Sal B are natural antioxidants that can protect human aortic endothelial cells against oxidative damage-mediated apoptosis through inhibiting the production of ROS [12-14]. Indeed, basic research on the compatibility of *Astragalus membranaceus* and *Salvia miltiorrhiza* in the treatment of AS is still at the beginning stage, and there are little studies concerning the combination of their effective monomers. According to online pharmacology, traditional prescriptions often exert multiple synergistic effects, such as synergistic interactions between herbs, effective parts, and pure compounds. It is also believed that synergistic effects between pure compounds are essential for the discovery of new drugs [15]. The nuclear factor-like 2 (Nrf2) can keep shuttling between the cytoplasm and the nucleus, and AsIV was found to inhibit the nuclear export of Nrf2 which was promoted by ferulic acid (FA). When FA and AsIV were activated in combination, their antioxidant effect was enhanced [16]. Therefore, we innovatively combine these two natural compounds to investigate whether they have synergistic effect on anti-oxidation and endothelial protection.

With the advent of the "omics" era, metabonomics become another new research tool after genomics, transcriptome and proteomics. It combines biogenetic changes to analyze all small molecules (molecular weight less than 1000 D) in cells, tissues and organs, and search for the corresponding biological targets and pathways to explain the biochemical state of organisms and the pathological mechanism of various complex traits [17], especially complex diseases such as AS [18, 19]. In the past, the development of TCM was hindered by the lack of suitable research tools. So far, there has been no related study concerning the effectiveness of AsIV, Sal B and their combination on AS by metabonomics technology. The liver is an important organ responsible for metabolic processes such as digestion, substance synthesis, decomposition and excretion of the human body [20, 21]. In particular, AS is a multi-factor and complex disease, characterized in abnormal lipid metabolism. As the main organ of material metabolism, the liver is involved in various metabolic changes in the body. Therefore, liver tissue is useful for metabolomics studies to analyze the final effect of drugs from the whole and multi-material levels. It is similar to the view of "holistic concept, dialectical treatment" of TCM, which bridges the research needs and available tools to describe the essence of TCM. It is of great significance to the innovative research and development of drugs in the future.

Materials and Methods

Animals and animal experiment

A total of 15 C57BL/6Cnc mice and 51 ApoE$^{-/-}$ mice (aged 8 weeks and weighing 19−21 g) were purchased from Beijing Weitong Lihua Experimental Animal Technology Co., Ltd. (Jinan, China). All the animals were maintained in the independent ventilation cages (IVC) of Shandong University of Traditional Chinese Medicine (under a 12/12 h of light/dark cycle, a 22−24 °C with a relative humidity of 50%−60%, laboratory animal license number: SCXK (Beijing)2016-0006). After acclimation for one week in normal fodders, only ApoE$^{-/-}$ mice were transferred to high fat fodders (78.85% basic feed, 21% fat, and 0.15% cholesterol) for 14 weeks. At the 14th week after model establishment, three mice were randomly selected from the normal group and the model group, respectively, and anesthetized with chloral hydrate (400 mg·kg^{-1}, i.p.). Blood samples were collected from the inferior vena cava, before rapid cardiac perfusion. After the mice were sacrifeid, biological tissue samples such as the heart and liver were collected. The abdominal aorta was stained with oil red O to determine whether the AS model was successfully established. Then, all mice were randomly divided into the following groups: a model group (M), an AsIV group, a Sal B group, and an AsIV combined with Sal B group (AsIV + Sal B), according to the random number table method, while wild-type C57BL/6Cnc mice were used as a control group (C). According to the ratio of equivalent conversion coefficient of 9.1 between mice and humans, mice in the AsIV group was administered with 4 mg·kg^{-1}·d^{-1} AsIV, the Sal B group was administered with 25 mg·kg^{-1}·d^{-1} Sal B, and the AsIV + Sal B group was administered with 4 mg·kg^{-1} AsIV + 25 mg·kg^{-1}·d^{-1} Sal B. The corresponding agents were given through intraperitoneal injection for 12 weeks. Meanwhile, the control and model groups were given an equal volume of normal saline by gavage for 12 weeks.

Drugs and reagents

Astragaloside IV was purchased from Shanghai Yuanye Biotechnology Co., Ltd. (Shanghai, China, No. 84687-43-4). Salvianolic acid B was purchased from Shanghai Yuanye Biotechnology Co., Ltd. (Shanghai, China, No. 115939-25-8). Oil red O dye solution was purchased from Beijing Dingsheng Changsheng Biotechnology Co., Ltd. (Beijing, China, DH222-1). The total superoxide dismutase (T-SOD) assay kit (A012-1), malondialdehyde (MDA) assay kit (A003-1), and nitric oxide (NO) assay kit (A001-1) were purchased from Nanjing Jiancheng Bioengineering Institute Co., Ltd. (Nanjing, China). Methanol, acetonitrile, ammonium acetate and ammonium hydroxide were purchased from CNW Technologies GmbH. 2-Chloro-L-phenylalanine was purchased from Shanghai Hengbai Biotechnology Co., Ltd. (Shanghai,

China).

Sample collection

After administration for continuous 12 weeks, the mice were anesthetized by intraperitoneal injection of chloral hydrate (400 mg·kg^{-1}, i.p.). Under aseptic conditions, the abdominal cavity was opened along the ventral midline, and the blood was taken from the inferior vena cava (about 1−2 mL of the blood was placed into a procoagulant tube). After placement at room temperature for 20 min, blood samples were centrifuged at 4 °C at 3500 r·min^{-1} for 15 min, and the supernatant was partially aspirated for the determination of SOD, MDA, and NO contents. The vessels from the aortic arch to the branches of the common iliac artery were dissected, washed with 0.9% normal saline for three times, and stored in 4% paraformaldehyde solution for fixation. Meanwhile, the remaining liver samples were obtained, in which part of the samples were frozen in liquid nitrogen for 30 s and stored at −80 °C for future metabolomics analysis.

Assessment of oxidative stress and endothelial protection

The aliquoted serum supernatant was aspirated to measure SOD, MDA, and NO contents by the corresponding kits (Nanjing Jiancheng Biochemical Co., Ltd., Nanjing, China), according to the manufacturer's instructions. SOD activity was measured by the xanthine oxidase method. MDA content was determined by thiobarbituric acid staining. NO content was determined using nitrate reductase.

Oil Red O staining of aorta

First, a working dye solution (1% oil red stock solution and 0.1% oil red working liquid) was prepared in advance. The aorta was longitudinally incised, rinsed with PBS for 3 min, soaked in 70% ethanol for 2 min, and stained with 0.1% oil red for 30 min. Then, the aorta was rinsed with 70% ethanol until the tissue became milky white, and then washed again with distilled water. The aorta was fixed on the foam plate and photographed. Finally, the red positive area within the plaque of each group was calculated by Image J.

Preparation of liver samples for metabolomics

First, 50 mg of the sample was weighed to put in 1000 μL of extraction solution (methanol : acetonitrile : water, 2 : 2 : 1) and mixed for 30 s, to which steel balls were added and ground for 4 min, followed by ice-water bath ultrasound for 5 min (repeated twice to three times). The sample was allowed to maintain at −40 °C for 1 h, before centrifugation at 4 °C at 10 000 r·min^{-1} for 15 min. The resultant supernatant (400 μL) was collected in an EP tube, to which 200 μL of 50% acetonitrile was added amd vortexed for 30 s ice-water bath ultrasound for 10 min. The samples were then centrifuged for another 15 min (4 °C, 13 000 r·min^{-1}). Then, 75 μL of the supernatant was collected for detection. In additiona, 10 μL of the supernatant was taken from all samples and mixed for quality control (QC), and the remaining samples to be tested were subject to LC-MS separation.

UPLC-QTOF-MS analysis

A 1290 Infinity Series UHPLC system (Agilent Technologies, USA) was used for UHPLC separation. The details were as follows: 95% B, 0−0.5 min; 95%−65% B, 0.5−7.0 min; 65%−40% B, 7.0−8.0 min; 40% B, 8.0−9.0 min; 40%−95% B, 9.0−9.1 min; and 95% B, 9.1−12.0 min. The column temperature was 25 °C. The auto-sampler temperature was 4 °C, and the injection volume was 1 μL (pos.) or 1 μL (neg.), respectively. Then, high-resolution mass spectrometry acquisition was performed on a Triple TOF 6600 high-resolution mass spectrometry platform. According to the preset scheme and the primary mass spectrometry data, the secondary mass spectrometry scan was automatically performed, the 12 ions with the highest intensity and > 100 per cycle were selected, and the collision energy of 30 eV and the cycle time of 0.56 s were selected. The ion source parameters were as follows: GS1, 60 psi; GS2, 30 psi; CUR, 35 psi; TEM, 600 °C; Dp, 60 V; and ISVF, 5000 V (pos)/−4000 V (Neg).

Statistical analysis

All data were expressed as the means ± SD (n = 10) and tested by SPSS 26.0 (SPSS Inc., Chicago, IL, USA). If the data satisfied the homogeneity of variance, SOD, MDA and NO were analyzed using the one-way analysis of variance (ANOVA), and Tukey HSD analysis was used for further pairwise comparison. If not, a nonparametric test was used. Metabolomics data were analyzed by t-test. Values of P < 0.05 were considered statistically different. Finally, all results were plotted by GraphPad Prism8 software.

Results

Results of oil red O staining

In order to evaluate the anti-AS effects of AsIV, Sal B and AsIV + Sal B, oil red O staining was performed on the aorta of mice in each group. As shown in Fig. 1, there was no obvious plaque in the whole vascular wall of the aorta in the control group, but a large number of plaques were attached to the intima in the model group, and the lumen of the aorta was blocked in the middle segment of the aorta. This finding is consistent with the results of many previous artificial models, which means that the animal model of AS was successfully established. AS mice were intraperitoneally injected with Sal B, AsIV or AsIV + Sal B for 12 weeks. Compared with the model group, the Sal B group, the AsIV group and the AsIV + Sal B group showed a significantly reduced plaque area. The plaque area of the AsIV + Sal B group significantly decreased, compared with those in the AsIV and Sal B groups (Fig. 1). These results demonstrated that AsIV, Sal B and AsIV + Sal B can reduce the area of plaque in the aorta of AS mice, with good therapeutic effect on AS disease.

Changes of serum SOD, MDA and NO contents

The SOD, MDA, and NO contents in the serum are shown in Table 1 and Fig. 2. Compared with the control group, the model group showed significant decreases in SOD activity and NO level, and increases in MDA level (P < 0.05). Compared with the model group, SOD activity and NO level increased, and MDA level decreased in each group. Specifically, SOD activity and NO content significantly increased,

while the level of MDA significantly decreased in the AsIV + Sal B group ($P < 0.01$). These results demonstrated that AsIV, Sal B and AsIV + Sal B can inhibit oxidative stress and protect vascular endothelial cells in AS mice, and AsIV + Sal B exhibit significant antioxidant and endothelial protective effects on AS disease.

Multivariate statistical analysis of metabolomics data

In the positive ion mode (Figs. 3A and 4A) and the negative ion mode (Fig. 3C and 4E), the results of principal component analysis (PCA) and orthogonal partial least squares discrimination analysis (OPLS-DA) score plots showed that the quality control (QC) samples had good clustering degree and concentrated in the 95% confidence interval, demonstrating that the experimental detection and analysis had good stability, and the resultant data were reliable. Samples in the model group were effectively separated from the control group, and the clustering of both groups performed well. The results implied that the liver metabolites of the model group were effectively separated and different from those of the normal group, demonstrating that the AS animal model was successfully established. Meanwhile, PCA (Figs. 3B and 3D) and OPLS-DA score plots (Figs. 4A, 4C, 4E and 4G) showed that the treatment groups were different from the model group, showing a separation trend. These data (Figs. 4B, 4D, 4F and 4H) suggested that the OPLS-DA models are reliable and valid.

Identification of differential metabolites

After OPLS-DA analysis, metabolites with VIP > 1.0 and $P < 0.05$ were selected as differential metabolites. Then, the differential metabolites were confirmed by the Human Metabolome Database (www.hmdb.ca), and the KEGG database (http://www.genome.jp/kegg/). Based on mass spectral fragmentation information, the exact mass and chemical structure of the selected metabolites in each group was identified.

Pathway analysis of differential metabolites

The differential metabolites identified in each group were compared, and the metabolic pathway invovled was obtained by MetaboAnalyst 4.0. The differential metabolites in the model group that had been identified were set as the comparison objects, and the potential biomarkers that were reversely changed after administration in the three groups were listed (Table 2). According to the disturbed metabolites, the changes of differential metabolites involved in the corresponding metabolic pathways were detected (Table 3). Based on the trend of metabolites and metabolic pathways, the relative changes among the four groups of metabolites were analyzed by hierarchical clustering with a heat map (Fig. 5). Bubble chart and horizontal bar chart were used to illustrate the relevant metabolic pathways in each group (Figs. 6 and 7). The changes of succinic acid and methionine metabolites were shown in each group (Fig. 8). Finally, an experimental flow chart (Fig. 9) was made in order to better explain the results.

Compared with the model group, three metabolites in the Sal B group were identified as differential metabolites, in which hydroxyproline, arginine, citrulline enriched arginine biosynthesis, arginine and proline metabolic pathway greatly changed (Tables 2 and 3, Fig. 6B). In the AsIV group, compared with the model group, eight metabolites were identified as differential metabolites, in which glycerol 3-phosphate enriched glycerol metabolic pathway, dodecanoic acid enriched fatty acid biosynthetic metabolic pathway and DL-2-aminoadipic acid enriched lysine degradation greatly changed (Tables 2 and 3, Fig. 6C). In the AsIV + Sal B group, compared with the model group, eight metabolites were identified as differential metabolites, in which succinic acid and *α*-ketoglutaricenriched enriched citric acid metabolic pathway (TCA cycle), succinic acid, *α*-ketoglutaric acid, aspartic acid and glutamate enriched alanine, aspartate and glutamate metabolism pathway, methionine enriched cysteine and methionine metabolism greatly changed (Tables 2 and 3, Fig. 6D). Compared with the group treated with Sal B or AsIV alone, the total metabolites and metabolic pathways significantly changed after administration of AsIV + Sal B, as reflected in TCA cycle and amino acid metabolism (Figs. 6 and 7). Among them, succinic acid and methionine were reversely changed metabolites in the AsIV + Sal B group, and the reverse trend was significantly stronger than administration of Sal B or AsIV alone (Fig. 8). It is suggested that succinic acid and methionine are the potential biomarkers of synergism.

Discussion

Anti-oxidant stress and vascular protection

The antioxidant properties and vasoprotective effects of AsIV and Sal B have been extensively investigated in previous research. But most studies were simply performed on single compounds *in vitro* and *in vivo* experiments to demonstrate their chemical properties and effects. In the current study, we found that AsIV + Sal B decreased SOD activity and MDA content, increased NO content, and significantly reduced plaque area in AS mice. Generally speaking, in the initial stage of AS, vascular endothelial cells can be activated by oxidative stress. Subendothelial low-density lipoprotein (LDL) is oxidized by lipoxygenase and reactive oxygen spe-

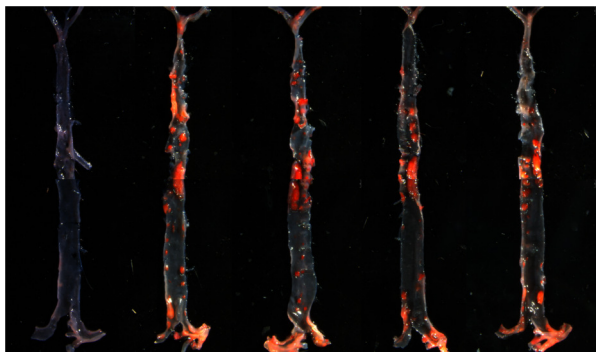

Fig. 1 Representative images of oil red O staining of the aorta in each group

Table 1 Changes of serum SOD, MDA and NO contents in each group (mean ± SD, $n = 8$)

Group	SOD (U·mL^{-1})	MDA (nmol·mL^{-1})	NO (μmol·mL^{-1})
Control	133.89 ± 11.05	3.39 ± 0.83	6.42 ± 1.67
Model	91.67 ± 11.01**	7.75 ± 1.24**	3.10 ± 1.47**
Sal B	108.70 ± 9.67$^{\#\#}$	4.56 ± 0.63$^{\#\#}$	4.01 ± 0.94
AsIV	100.37 ± 5.84	6.16 ± 0.95$^{\#}$	4.28 ± 2.16
AsIV + Sal B	111.05 ± 8.12$^{\#\#}$	4.86 ± 0.86$^{\#\#}$	5.00 ± 1.29$^{\#}$

$^{*}P < 0.05$, $^{**}P < 0.01$ *vs* the control group; $^{\#}P < 0.05$, $^{\#\#}P < 0.01$ *vs* the model group

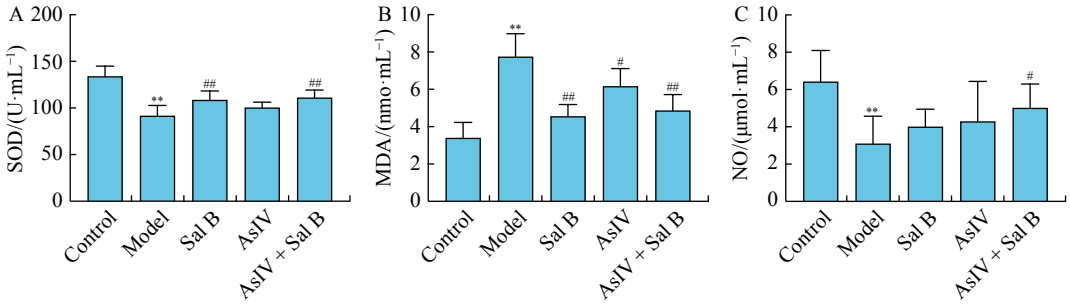

Fig. 2 After intervention with Sal B, AsIV or AsIV + Sal B for 14 weeks, the changes of serum SOD, MDA and NO contents in each group are shown in A, B, C. Data are expressed as the mean ± SD ($n = 8$); $^{**}P < 0.01$ *vs* the control group; $^{\#}P < 0.05$, $^{\#\#}P < 0.01$ *vs* the model group

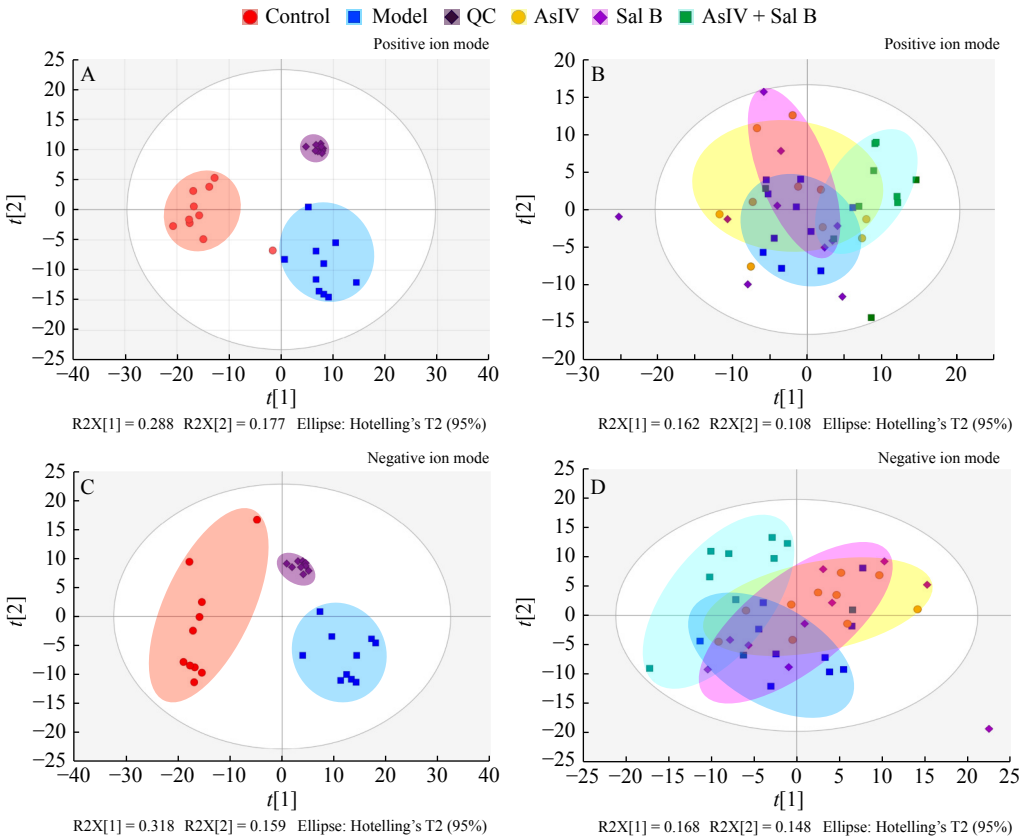

Fig. 3 PCA statistical analysis of liver data. A: PCA score plots of the control group, the model group and quality control (QC) samples in a positive ion mode. B: PCA score plots of the model group, the AsIV group, the Sal B group, and the AsIV + Sal B group in a positive ion mode. C: PCA score plots of the control group, the model group and QC samples in a negative ion mode. D: PCA score plots of the model group, the AsIV group, the Sal B group and the AsIV + Sal B group in a negative ion mode

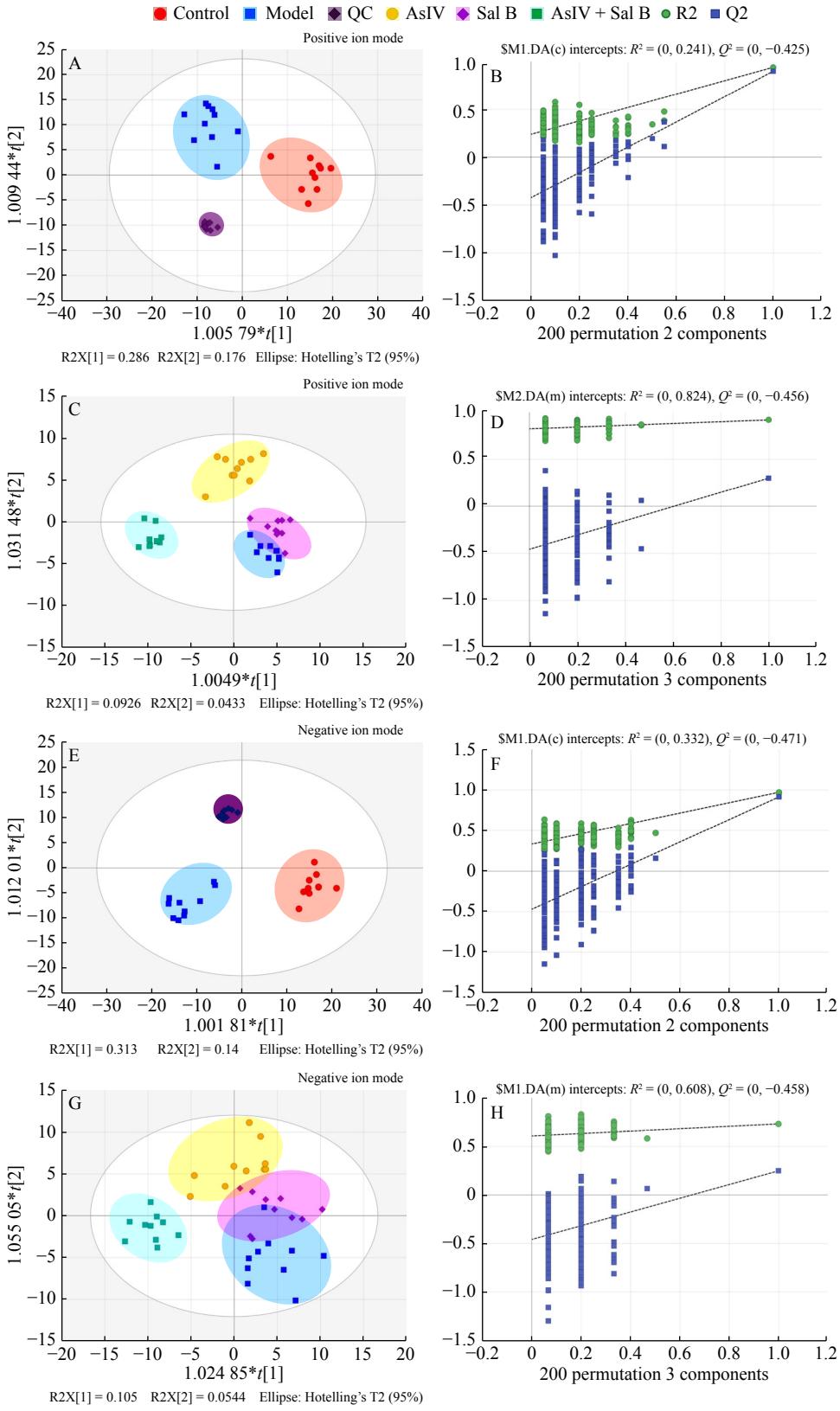

Fig. 4 OPLS-DA statistical analysis of liver data. A and B: OPLS-DA and permutation score plots of the control group, the model group and quality control (QC) samples in a positive ion mode. C and D: OPLS-DA and permutation score plots of the model group, the AsIV group, the Sal B group, and the AsIV + Sal B group in a positive ion mode. E and F: OPLS-DA and permutation score plots of the control group, the model group and QC samples in a negative ion mode. G and H: OPLS-DA and permutation score plots of the model group, the AsIV group, the Sal B group, and the AsIV + Sal B group in a negative ion mode

cies to generate OX-LDL. On the contrary, lipid peroxidation can easily increase the ROS of reactive oxygen clusters. When it exceeds the endogenous antioxidant response balance system in the body, endothelial injury will be induced, which greatly accelerates the formation of plaques and the development of AS [22, 23]. Therefore, MDA, a peroxidation product produced by lipid peroxidation, is often used as an indicator to evaluate the degree of oxidative damage in AS. However, SOD can catalyze the dismutation of superoxide anion radicals to generate oxygen and hydrogen peroxide, maintain the production and inactivation of oxygen free radicals, and protect cell membranes against damage [24]. NO easily affects endothelial cell-derived contractile factors, thereby regulating vascular tension, inhibiting platelet aggregation, and protecting endothelial cells [25, 26]. Obviously, these factors must be controlled and prevented to inhibit the development of AS. The selection of SOD, MDA, and NO can comprehensively assess the antioxidant capacity of organisms and the protective effect of vascular endothelium. During the pathogenesis of AS, AsIV + Sal B showed the same or even stronger antioxidant and vasoprotective ability in these indicators, compared with the monotherapy groups. This is consistent with our expected results, and also provides a theoretical basis for AsIV + Sal B to exert antioxidant and vascular protective effects. Clearly, the underlying mechanisms of action requires further exploration.

Metabolomics analysis

First, we used metabolomics technology to obtain the small molecular metabolites that affect AS in each group. Compared with the model group, hydroxyproline, which originally increased, showed a decreasing trend after administration of Sal B, and the levels of citrulline and arginine were also down-regulated. These changes disturbed the metabolism of arginine and proline and the pathway of arginine biosynthesis. Hydroxyproline is a product of posttranslational hydroxylation of proline catalyzed by proline hydroxylase [27], and proline is unique amino acids in collagen. Collagen is a structural protein, which plays an important role in controlling the mechanical property of blood vessels. If any factor (including oxidative stress and inflammatory factors) stimulates the synthesis and secretion of collagen in the arterial wall, collagen will deposit within the arterial wall and participate in the pathogenesis of AS [28]. Therefore, hydroxyproline can be used not only as a measurement of collagen or collagen degradation products in serum or tissue [29], but also as a biological indicator of oxidative stress and inflammatory reaction in tissue [30]. Citrulline and arginine are the intermediate metabolites of the urea cycle. Citrulline is produced by ornithine and carbamyl phosphate in the urea cycle, or when arginine is catalyzed by nitric oxide synthase (NOS) to produce NO. Arginine is the only precursor for the synthesis of NO in the body. In addition, citrulline can enter the cyto-

Table 2 Potential biomarkers identified in each group (mean ± SD, n = 10)

Biomarkers	*m/z*	t_R/min	M/C				Sal B/M				AsIV/M				(AsIV + Sal B)/M			
			VIP	*P*	FC	CT	VIP	*P*	FC	CT	VIP	*P*	FC	CT	VIP	*P*	FC	CT
Succinic acid	259.04	155.45	1.65	0.001	5.91	↑	-	-	-	-	-	-	-	-	1.1	0.025	0.5	↓
Dodecanoic acid	199.17	47.07	1.61	0	2.07	↑	-	-	-	-	1.9	0.006	0.7	↓	-	-	-	-
Linoleoyl ethanolamide	324.29	35.64	1.38	0	1.96	↑	-	-	-	-	1.53	0.03	0.69	↓	-	-	-	-
Hydroxyproline	114.05	287.53	1.74	0	1.92	↑	2.4	0.027	0.82	↓	-	-	-	-	-	-	-	-
alpha-Guanidinoglutaric Acid	250.11	379.78	1.47	0.001	1.66	↑	-	-	-	-	2.88	0.001	0.61	↓	1.39	0.008	0.72	↓
β-Homoproline	130.09	310.33	1.14	0.008	1.63	↑	-	-	-	-	2.3	0.009	0.63	↓	1.5	0.015	0.65	↓
5,2′-*O*-Dimethylcytidine	332.14	356.14	1.27	0.005	1.46	↑	2.5	0.001	0.61	↓	2.52	0.025	0.53	↓	1.48	0.009	0.72	↓
L-Methionine	148.04	287.58	1.11	0.007	0.61	↓	-	-	-	-	-	-	-	-				↑
N-Acetyl-D-glucosamine	186.08	468.14	1.57	0	0.59	↓	-	-	-	-	-	-	-	-	1.53	0.015	1.36	↑
Purine	119.03	161.8	1.35	0	0.53	↓	2.8	0.008	1.46	↑	-	-	-	-	1.88	0	1.88	↑
Monomethyl glutaric acid	183.01	161.62	1.31	0.003	0.52	↓	2.82	0.007	1.45	↑	-	-	-	-	-	-	-	-
Glycerol 3-phosphate	171.01	415.66	1.2	0.003	0.48	↓	-	-	-	-	1.62	0.047	1.38	↑	-	-	-	-
1-Oleoyl-sn-glycerol 3-phosphate	457.23	172.71	1.4	0	0.47	↓	-	-	-	-	-	-	-	-	1.49	0.011	1.51	↑
DL-2-Aminoadipic acid	162.07	388.76	1.64	0	0.4	↓	-	-	-	-	1.95	0.034	6.32	↑	-	-	-	-
Phenylacetylglycine	252.09	197.59	1.49	0.048	0.22	↓	-	-	-	-	-	-	-	-	1.12	0.016	1.69	↑

M/C indicates the model group (M) compared with the control group (C); Sal B/M indicates the Sal B group (Sal B) compared with the model group (M); AsIV/M indicates the AsIV group (AsIV) compared with the model group (M); (AsIV + Sal B)/M indicates the AsIV + Sal B group (AsIV + Sal B) compared with the model group (M); (↑): up-regulated; (↓): down-regulated; $P < 0.01$ *vs* the model group. *m/z*: mass to charge ratio; t_R: retention time; VIP: variable importance projection; FC: fold change; CT: change trend

Table 3 Potential biomarkers in the corresponding metabolic pathways

Pathway	M/C	Sal B/M	AsIV/M	(AsIV + Sal B)/M
Citrate cycle (TCA cycle)	Succinate↑	-	-	Succinate↓; 2-Oxoglutarate↑
Alanine, aspartate and glutamate metabolism	L-Glutamine↓;Succinate↑	-	-	Succinate↓;D-Aspartate↑; L-Glutamate↑;2-Oxoglutarate↑;
Cysteine and methionine metabolism	L-Methionine↓;L-Cystine↑	-	-	L-Methionine↑;L-Cystine↑; L-Serine↑
D-Glutamine and D-glutamate metabolism	L-Glutamine↓	-	-	2-Oxoglutarate↑; L-Glutamate↑
Amino sugar and nucleotide sugar metabolism	*N*-Acetyl-D-glucosamine↓;D-Galactose↓	-	-	*N*-Acetyl-D-glucosamine↑;D-Galactose↓
Phenylalanine metabolism	L-Tyrosine↓; Phenylacetylglycine↓	-	-	Phenylacetylglycine↑; Phenylalanine↑
Arginine and proline metabolism	Hydroxyproline↑	Hydroxyproline↓; Arginine↓	-	-
Arginine biosynthesis	L-Glutamine↓	Arginine↓; Citrulline↓	-	2-Oxoglutarate↑; L-Glutamate↑
Fatty acid biosynthesis	Dodecanoic acid↑	-	Dodecanoic acid↓	-
Glycerolipid metabolism	Glycerol 3-phosphate↓	-	Glycerol 3-phosphate↑	-
Lysine degradation	DL-2-Aminoadipic acid↓	-	DL-2-Aminoadipic acid↑	-
Glycerophospholipid metabolism	Glycerol 3-phosphate↑;	-	Glycerol 3-phosphate↑;	-

M/C indicates the model group (M) compared with the control group (C); Sal B/M indicates the Sal B group (Sal B) compared with the model group (M); AsIV/M indicates the AsIV group (AsIV) compared with the model group (M); (AsIV + Sal B)/M indicates the AsIV + Sal B group (AsIV + Sal B) compared with the model group (M); (↑): up-regulated; (↓): down-regulateds

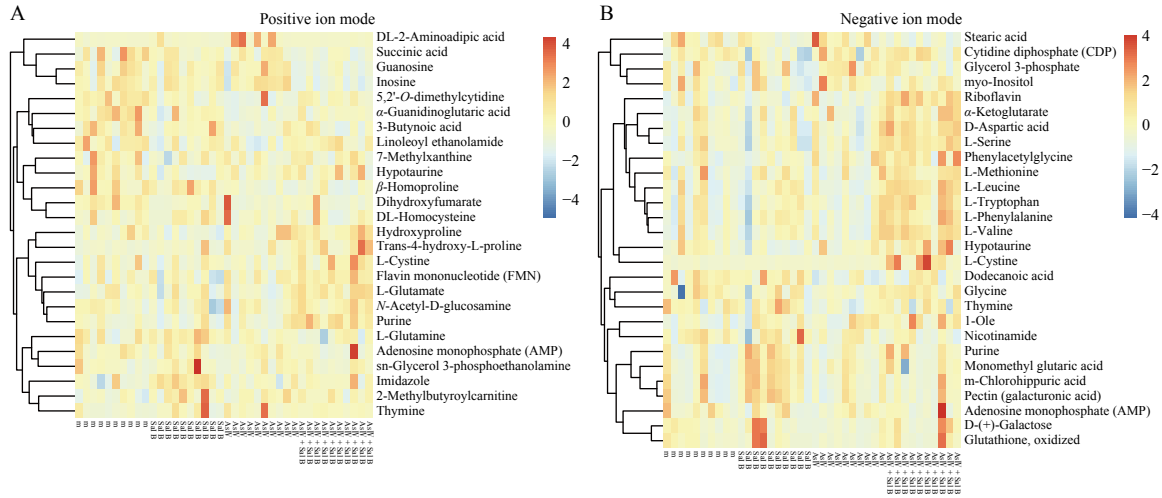

Fig. 5 Heat map of 26 differentially produced endogenous metabolites in the model group, the Sal B group, the AsIV group and the AsIV + Sal B group. Red plots indicate up-regulated metabolites, and blue plots indicate down-regulated metabolites in rats. A stands for a positive ion mode, and B stands for a negative ion mode

plasm through the mitochondrial membrane, and the urea group of citrulline is condensed with the amino group of aspartic acid catalyzed by arginine succinate synthetase to form arginine succinic acid. Arginine succinic acid is then catalyzed by arginine succinic acid lyase to produce arginine and fumaric acid. In this experiment, the content of hydroxyproline in the model group was up-regulated, indicating that collagen may deposit in the intima of the artery wall and the mechanical support characteristics of the blood vessels were weakened.

We observed that the content of glycerol-3-phosphate, which showed a decreasing trend in the model group, turned into an increasing trend in the AsIV group. The contents of dodecanoic acid, linoleamide and α-argarinic acid, which originally showed an increasing trend, turned into a decreasing trend after administration in the AsIV group. The changes disturbed the glycerol metabolism, fatty acid biosynthesis pathway. Triglycerides decompose *in vivo* to produce glycer-

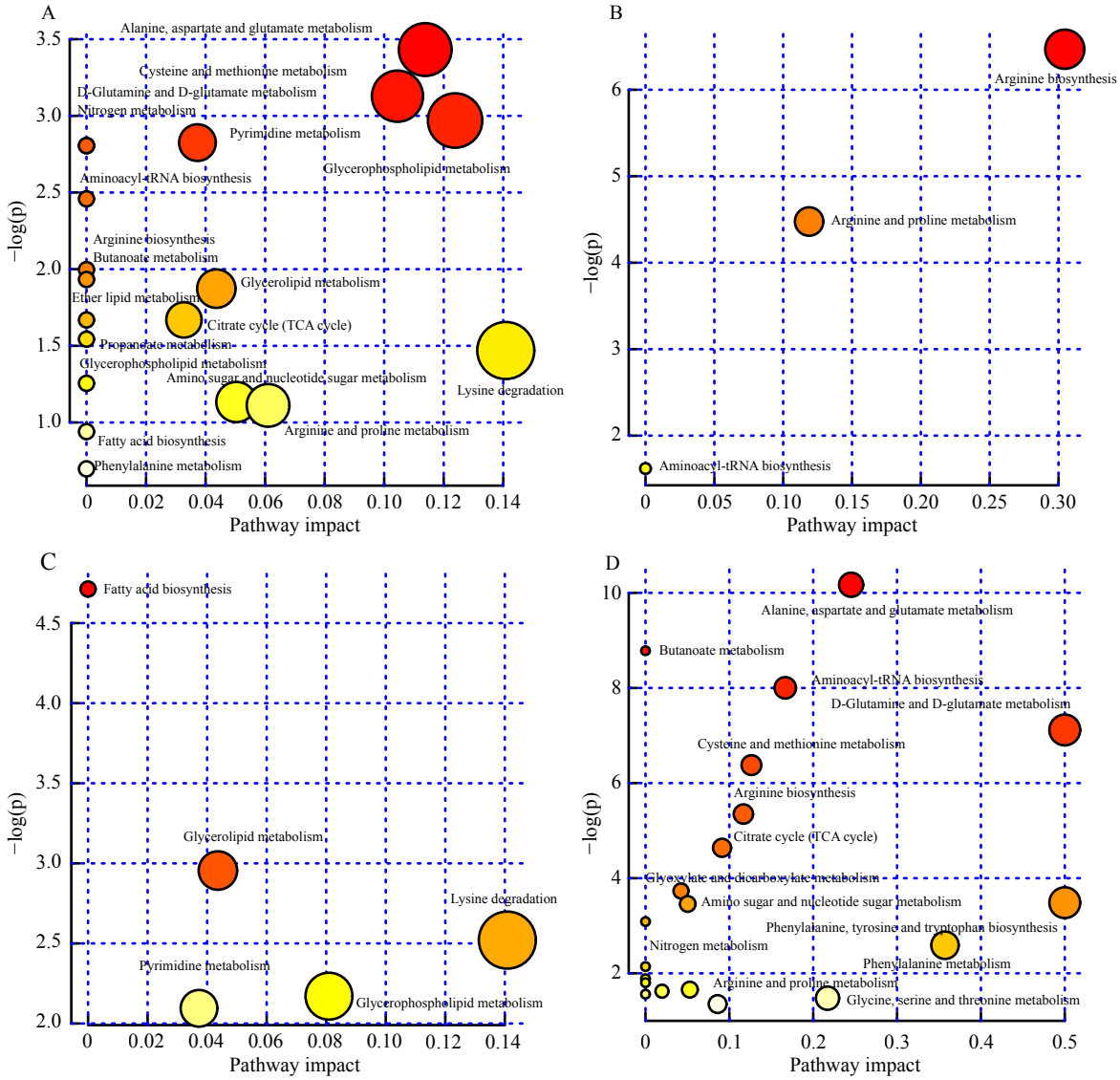

Fig. 6 Disturbed metabolic pathways showed various metabolism changes by bubble chart, when comparing the control group to the model group (A), the model group to the Sal B group (B), the model group to the AsIV group (C), the model group to the AsIV + Sal B group (D)

ol and fatty acids, and then glycerol is phosphorylated by glycerol kinase to form glycerol-3-phosphate, and oxidized and dehydrogenated to dihydroxyacetone phosphate (DHAP) by glycerol phosphate dehydrogenase. DHAP is the intermediate of glycerol allogenic sugar, which is at the intersection of glucose and fat metabolism. DHAP is converted to glyceraldehyde-3-phosphate by triose phosphate isomerase, which participates in the subsequent cycle of gluconeogenesis and energy metabolism among substrates [31]. Dodecanoic acid is a saturated fatty acid in the body and one of the main risk factors for AS. Studies have shown that the content of dodecanoic acid is positively correlated with the content of serum cholesterol [32]. *α*-Guanidoglutaric acid is a derivative of glutamic acid. Studies have shown that *α*-guanidoglutaric acid can be used as a new nitric oxide synthase (NOS) [33] inhibitor to suppress the release of NO, where NOS is the most important rate-limiting factor for NO production [34]. Therefore, it is speculated that AsIV may provide energy for the body by promoting the conversion of glycerol components to glucose or participating in the tricarboxylic acid cycle, inhibiting the synthesis of saturated fatty acids that are bad for the body, and reducing related molecules that affect the state of vascular endothelium. It is suggested that AsIV regulates the related energy metabolism, lipid metabolism and vascular endothelial state, It plays an important role in antioxidant stress and endothelial protection in AS mice.

After administration of AsIV + Sal B, succinic acid, which showed a decreasing trend in AS mice, turned into an increasing trend, while methionine content with an originally increasing trend turned into a decreasing trend. These changes interfered with TCA cycle, alanine, aspartic acid and glutamate metabolism and cysteine and methionine metabol-

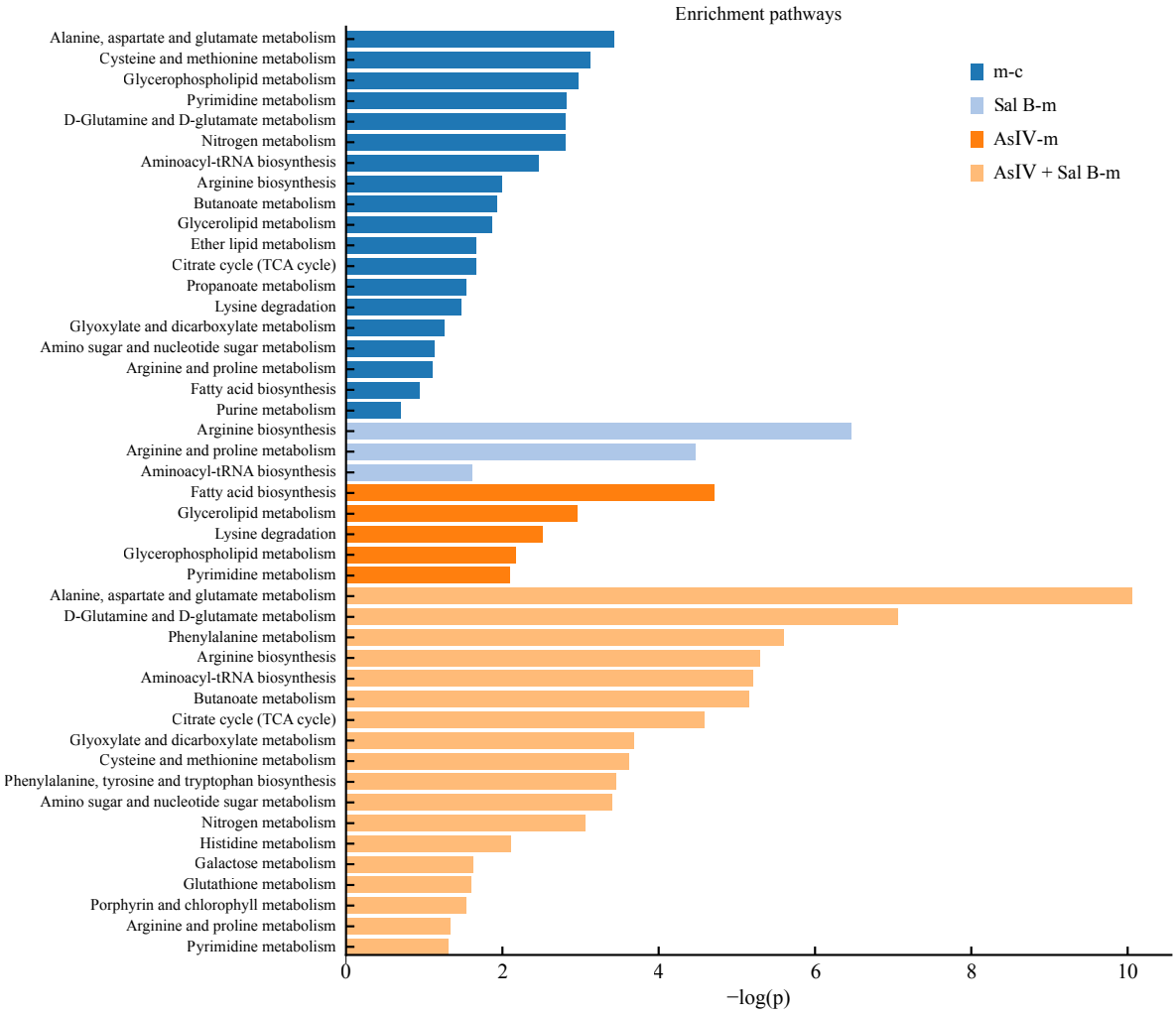

Fig. 7 Disturbed metabolic pathways showed various metabolism changes by bar histogram, when comparing the control group to the model group (A), the model group to the Sal B group (B), the model group to the AsIV group and (C), the model group to the AsIV + Sal B group (D)

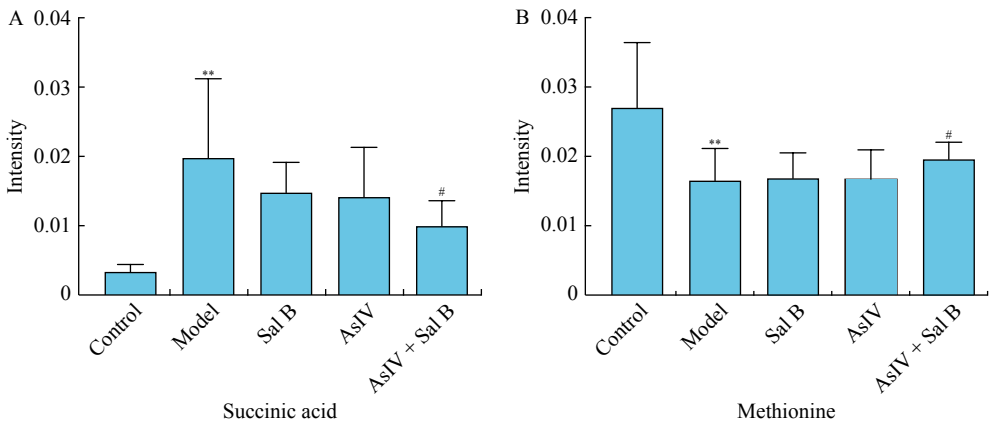

Fig. 8 After intervention of Sal B, AsIV, or AsIV + Sal B for 12 weeks, the changes of succinic acid and methionine metabolites in the control group, the model group, the Sal B group, the AsIV group and the AsIV + Sal B group are shown in A and B. Data are expressed as the mean ± SD (n = 10); $^{**}P < 0.01$ *vs* the control group; $^{\#}P < 0.05$, $^{\#\#}P < 0.01$ *vs* the model group

ism pathway. Normally, succinic acid acts as an intermediate in the TCA cycle in mitochondria and participates in energy metabolism. However, the degree of its accumulation in the body is a common metabolic feature of tissue ischemia, which helps to increase the level of ROS [35]. In the Leite [36] study, it was shown that different concentrations of succinic

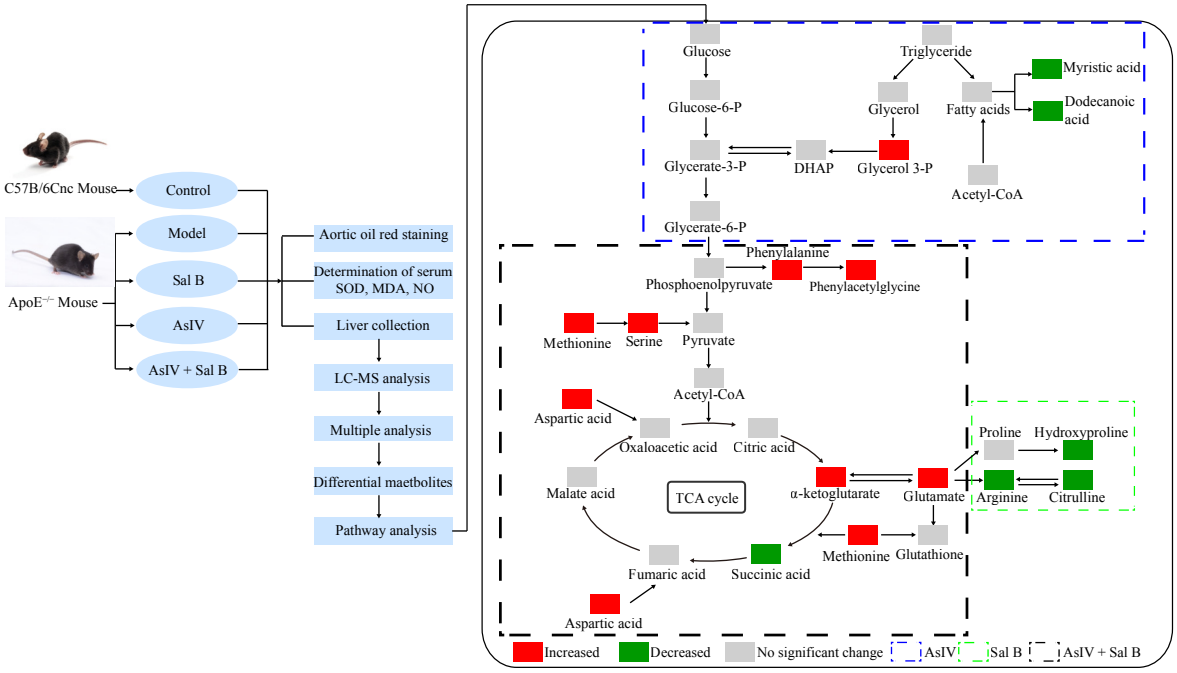

Fig. 9 Experimental flow chart of the morphological, antioxidant and antivascular protection indexes and liver metabolomics approaches

acid directly exerted two-way effect on the vessels *via* the endothelial GPR91 receptor, where the NO-cGMP pathway mediated by the vasodilator plus oxygenase (COX) and potassium (K^+) channel was opened. If its concentration is low, the blood vessel will relax, and a high concentration may result in opposite effect. Therefore, its abnormal changes indicate mitochondrial damage and dysfunction, which is related to oxidative stress and vascular endothelial protection. When AsIV + Sal B was administered, the succinate content decreased, which indicated that the mechanism by which AsIV + Sal B function against AS is likely to achieve through regulating the TCA circle, espeically promoting mitochondrial production and release of ATP, restoring mitochondrial injury and dysfunction, reducing the secretion of ROS and inflammatory factors, and protecting vascular endothelium from inflammatory and oxidative stress damage.

Methionine is an essential amino acid and contains sulfide similar to cystine and cysteine [37]. The -SH structure can not only enhance the activity of glutathione peroxidase and SOD, but also contribute to the synthesis of endogenous antioxidant glutathione. Its methylation can promote the synthesis of endogenous phospholipids and protect cardiomyocytes against mitochondrial damage, so as to protect cardiovascular disease [38]. As a result, lipid overoxidation, inflammatory reaction and vascular endothelial dysfunction in AS are closely related to the cysteine and methionine metabolism pathway. Furthermore, an increased methionine content in the body inhibited fat accumulation, enhanced immune responses and improved antioxidant capacity [39]. This means that AsIV + Sal B can inhibit lipid peroxidation and reduce the damage of important organelles such as mitochondria through exhibiting antioxidant effects in AS mice. In addition, AsIV + Sal B also resulted in significant increases in cystine contents. Methionine can be converted to cysteine. Cysteine and cystine can be interchangeable, but neither can generate methionine [37]. It is speculated that the content of methionine increased and the conversion between cystine and cysteine is promoted because after administration, the activity of glutathione peroxidase and SOD are enhanced by the -SH structure, which is helpful for the synthesis of glutathione. This explains the changes of SOD, MDA, and NO in the first part of the experiment. It was intended to show that the mechanism of action of AsIV + Sal B against AS is closely related to this pathway. Moreover, methionine and succinic acid showed a reverse trend ($P > 0.05$) in the Sal B and AsIV groups alone. But when the two monomers were used in combination, the reverse trend reached a significant difference ($P < 0.05$), suggesting that the monomers used in combination exert a synergistic effect. This is consistent with the function of anti-oxidation, protecting vascular endothelial cells and reducing aortic plaque after the combined use of the two monomers in the first part of the experiment. The analysis showed that succinate and methionine are the most potential biomarker, involving the TCA cycle, alanine, aspartic acid and glutamate metabolism and cysteine and methionine metabolism pathways.

Conclusion

In this study, we investigated the metabolism of endogenous small molecules of AS based on the combination of UPLC-Q/TOF-MS metabonomics with aortic staining and serological indexes, so as to evaluate the antioxidant and vascular protective mechanisms of Sal B, AsIV and AsIV + Sal B in ApoE$^{-/-}$ mice induced by high-fat diet. Then, the lipid plaque deposition, SOD activity, and MDA and NO contents in the aorta of AS model mice were evaluated. Results

showed that Sal B, AsIV and AsIV + Sal B exhibited a reverse effect, and the reverse effect of AsIV + Sal B was the most obvious, which demonstrated that AsIV + Sal B exhibite good antioxidant and vascular protection effects. Metabonomic analysis showed that three differential metabolites in the Sal B group significantly changed compared with the model group. It is speculated that hydroxyproline, citrulline and proline can be used as the potential biomarkers of antioxidation and endothelial protection and are related to the regulation of arginine and proline metabolic pathway. Eight differential metabolites significantly changed in the AsIV group. It is speculated that glycerol-3-phosphate, dodecanoic acid and α-guanidine glutaric acid regulate glycerol metabolism saturated fatty acid biosynthesis metabolism, play a role in antioxidant stress and endothelial protection and can be used as potential biomarkers. There were significant changes in the levels of eight related differential metabolites in the AsIV + Sal B group. It is speculated that succinic acid and methionine can be used as potential biomarkers of antioxidation and endothelial protection, which are related to the regulation of TCA cycle, alanine, aspartic acid and glutamate metabolism and cysteine and methionine metabolism pathway. In particular, succinic acid and methionine can also be used as co-metabolites of AsIV and Sal B, suggesting that AsIV + Sal B can enhance the antioxidant and vascular protective effects of Sal B and AsIV alone. Therefore, based on metabolomic data, we preliminarily elucidated the antioxidant and vasoprotective mechanisms of Sal B, AsIV and AsIV + Sal B in the treatment of AS, where AsIV + Sal B was more effective than AsIV and Sal B alone and functioned a synergistic manner. Meanwhile, the discovery of potential biomarkers that play a synergistic role can provide a certain theoretical and experimental basis for the future development of natural medicines in China.

References

[1] Organization WH. Cardiovascular diseases (CVDs) [EB/OL]. https://www.who.int/news-room/fact-sheets/detail/cardiovascular-diseases-(cvds), 2021-6-11.

[2] Teo KK, Dokainish H. The emerging epidemic of cardiovascular risk factors and atherosclerotic disease in developing countries [J]. *Can J Cardiol*, 2017, **33**(3): 358-365.

[3] Bentzon JF, Otsuka F, Virmani R, *et al*. Mechanisms of plaque formation and rupture [J]. *Circ Res*, 2014, **114**(12): 1852-1866.

[4] Burtenshaw D, Kitching M, Redmond EM, *et al*. Reactive oxygen species (ROS), intimal thickening, and subclinical atherosclerotic disease [J]. *Front Cardiovasc Med*, 2019, **6**: 89.

[5] Shimokawa H, Godo S. Nitric oxide and endothelium-dependent hyperpolarization mediated by hydrogen peroxide in health and disease [J]. *Basic Clin Pharmacol Toxicol*, 2020, **127**(2): 92-101.

[6] Battelli MG, Polito L, Bolognesi A. Xanthine oxidoreductase in atherosclerosis pathogenesis: not only oxidative stress [J]. *Atherosclerosis*, 2014, **237**(2): 562-567.

[7] Gimbrone MA, García-Cardeña G. Endothelial cell dysfunction and the pathobiology of atherosclerosis [J]. *Circ Res*, 2016, **118**(4): 620-636.

[8] Xu Q, Bauer R, Hendry BM, *et al*. The quest for modernisation of traditional Chinese medicine [J]. *BMC Complement Altern Med*, 2013, **13**: 132.

[9] Liu Y, Xue Q, Li A, *et al*. Mechanisms exploration of herbal pair of HuangQi-DanShen on cerebral ischemia based on metabonomics and network pharmacology [J]. *J Ethnopharmacol*, 2020, **253**: 112688.

[10] Han C, Jiang YH, Li W, *et al*. Study on the antihypertensive mechanism of *Astragalus membranaceus* and *Salvia miltiorrhiza* based on intestinal flora-host metabolism [J]. *Evid Based Complement Alternat Med*, 2019, **2019**: 5418796.

[11] Han JY, Li Q, Pan CS, *et al*. Effects and mechanisms of QiShenYiQi pills and major ingredients on myocardial microcirculatory disturbance, cardiac injury and fibrosis induced by ischemia-reperfusion [J]. *Pharmacol Res*, 2019, **147**: 104386.

[12] Zhu Z, Li J, Zhang X. Astragaloside IV protects against oxidized low-density lipoprotein (ox-LDL)-induced endothelial cell injury by reducing oxidative stress and inflammation [J]. *Med Sci Monit*, 2019, **25**: 2132-2140.

[13] Zhang J, Wu C, Gao L, *et al*. Astragaloside IV derived from *Astragalus membranaceus*: a research review on the pharmacological effects [J]. *Adv Pharmacol*, 2020, **87**: 89-112.

[14] Yang TL, Lin FY, Chen YH, *et al*. Salvianolic acid B inhibits low-density lipoprotein oxidation and neointimal hyperplasia in endothelium-denuded hypercholesterolaemic rabbits [J]. *J Sci Food Agric*, 2011, **91**(1): 134-141.

[15] Yuan H, Ma Q, Cui H, *et al*. How can synergism of traditional medicines benefit from network pharmacology [J]. *Molecules*, 2017, **22**(7): 1135.

[16] Liang Y, Zou Y, Niu C, *et al*. Astragaloside IV and ferulic acid synergistically promote neurite outgrowth through Nrf2 activation [J]. *Mech Ageing Dev*, 2019, **180**: 70-81.

[17] Nicholson JK, Wilson ID. Opinion: understanding "global" systems biology: metabonomics and the continuum of metabolism [J]. *Nat Rev Drug Discov*, 2003, **2**(8): 668-676.

[18] Tzoulaki I, Castagné R, Boulangé CL, *et al*. Serum metabolic signatures of coronary and carotid atherosclerosis and subsequent cardiovascular disease [J]. *Eur Heart J*, 2019, **40**(34): 2883-2896.

[19] Iida M, Harada S, Takebayashi T. Application of metabolomics to epidemiological studies of atherosclerosis and cardiovascular disease [J]. *J Atheroscler Thromb*, 2019, **26**(9): 747-757.

[20] Heindel JJ, Blumberg B, Cave M, *et al*. Metabolism disrupting chemicals and metabolic disorders [J]. *Reprod Toxicol*, 2017, **68**: 3-33.

[21] Ponziani FR, Pecere S, Gasbarrini A, *et al*. Physiology and pathophysiology of liver lipid metabolism [J]. *Expert Rev Gastroenterol Hepatol*, 2015, **9**(8): 1055-1067.

[22] Balzan S, Lubrano V. LOX-1 receptor: a potential link in atherosclerosis and cancer [J]. *Life Sci*, 2018, **198**: 79-86.

[23] Hartley A, Haskard D, Khamis R. Oxidized LDL and anti-oxidized LDL antibodies in atherosclerosis: novel insights and future directions in diagnosis and therapy [J]. *Trends Cardiovasc Med*, 2019, **29**(1): 22-26.

[24] Fukai T, Ushio-Fukai M. Superoxide dismutases: role in redox signaling, vascular function, and diseases [J]. *Antioxid Redox Signal*, 2011, **15**(6): 1583-1606.

[25] Förstermann U, Xia N, Li H. Roles of vascular oxidative stress and nitric oxide in the pathogenesis of atherosclerosis [J]. *Circ Res*, 2017, **120**(4): 713-735.

[26] Ho E, Karimi Galougahi K, Liu CC, *et al*. Biological markers of oxidative stress: applications to cardiovascular research and practice [J]. *Redox Biol*, 2013, **1**(1): 483-491.

[27] Pihlajaniemi T, Myllylä R, Kivirikko KI. Prolyl 4-hydroxylase and its role in collagen synthesis [J]. *J Hepatol*, 1991, **13**(Suppl 3): S2-S7.

[28] Abdelhalim MAK, Siddiqi NJ, Alhomida AS, *et al*. The changes in various hydroxyproline fractions in aortic tissue of rabbits are closely related to the progression of atherosclerosis [J]. *Lipids in health and disease*, 2010, **9**: 26.

[29] Duprez DA, Gross MD, Sanchez OA, *et al*. Collagen turnover markers in relation to future cardiovascular and noncardiovascular disease: the multi-ethnic study of atherosclerosis [J]. *Clin Chem*, 2017, **63**(7): 1237-1247.

[30] Srivastava AK, Khare P, Nagar HK, *et al*. Hydroxyproline: a potential biochemical marker and its role in the pathogenesis of different diseases [J]. *Curr Protein Pept Sci*, 2016, **17**(6): 596-602.

[31] Jang M, Kang HJ, Lee SY, *et al*. Glyceraldehyde-3-phosphate, a glycolytic intermediate, plays a key role in controlling cell fate *via* inhibition of caspase activity [J]. *Mol Cells*, 2009, **28**(6): 559-563.
[32] Qureshi W, Santaren ID, Hanley AJ, *et al*. Risk of diabetes associated with fatty acids in the de novo lipogenesis pathway is independent of insulin sensitivity and response: the Insulin Resistance Atherosclerosis Study (IRAS) [J]. *BMJ Open Diabetes Res Care*, 2019, **7**(1): e000691.
[33] Habu H, Yokoi I, Kabuto H, *et al*. Seizures induced by alpha-guanidinoglutaric acid, a nitric oxide synthase inhibitor, are controlled by L-arginine [J]. *Biochem Mol Biol Int*, 1996, **39**(1): 87-95.
[34] Tsutsui M, Shimokawa H, Otsuji Y, *et al*. Pathophysiological relevance of NO signaling in the cardiovascular system: novel insight from mice lacking all NO synthases [J]. *Pharmacol Ther*, 2010, **128**(3): 499-508.
[35] Andrienko TN, Pasdois P, Pereira GC, *et al*. The role of succinate and ROS in reperfusion injury: a critical appraisal [J]. *J Mol Cell Cardiol*, 2017, **110**: 1-14.
[36] Leite LN, Gonzaga NA, Simplicio JA, *et al*. Pharmacological characterization of the mechanisms underlying the vascular effects of succinate [J]. *Eur J Pharmacol*, 2016, **789**: 334-343.
[37] Brosnan JT, Brosnan ME. The sulfur-containing amino acids: an overview [J]. *J Nutr*, 2006, **136**(6 Suppl): 1636s-1640s.
[38] Guo T, Chang L, Xiao Y, *et al*. *S*-adenosyl-L-methionine for the treatment of chronic liver disease: a systematic review and meta-analysis [J]. *PLoS One*, 2015, **10**(3): e0122124.
[39] Aledo JC. Methionine in proteins: the cinderella of the proteinogenic amino acids [J]. *Protein Sci*, 2019, **28**(10): 1785-1796.

Cite this article as: KONG Xiang-Lin, LYU Qin, ZHANG Ya-Qi, KANG Dong-Fang, LI Chao, ZHANG Lei, GAO Zi-Chen, LIU Xin-Xin, WU Ji-Biao, LI Yun-Lun. Effect of astragaloside IV and salvianolic acid B on antioxidant stress and vascular endothelial protection in the treatment of atherosclerosis based on metabonomics [J]. *Chin J Nat Med*, 2022, **20**(8): 601-613.